DATA ASSIMILATION (4D-VAR) FOR SHALLOW-WATER FLOW: THE CASE OF THE CHICOUTIMI RIVER

Eric Bélanger, Alain Vincent, Alexandre Fortin
Centre de Recherche en Calcul Appliqué (CERCA)
5160, boul. Décarie, bureau 400
Montréal, QC
H3X 2H9
belanger@CERCA.UMontreal.CA, vincent@CERCA.UMontreal.CA
fortina@CERCA.UMontreal.CA

Abstract

Data assimilation is a method which is needed to make more accurate short term forecast. We explain the 4D-VAR technique and apply it to the shallow-water equations. We tested the method in a degradation case and found that the 4D-VAR effectively reduces the error between the results of the simulation and the observations.

1 INTRODUCTION

A river bed is an active medium which can be degraded in the course of time. A river whose bed is too weakened can even, in the event of abundant precipitation, brutally change its course [1].

In the month of July 1996, an important rainstorm hit the region of Saguenay in Québec which received over 200 mm of rain over the next 36 hours [2]. This large amount of water, on the already saturated ground, increased the discharge of several tributaries of the Saguenay River thus creating severe flooding in the area [3].

One example of degradation is the bypass of the Chute-Garneau dam [4]. The water accumulated and started spilling over the dam because some of the sluice gates were malfunctioning or blocked by floating debris. Furthermore, an incision began in the unconsolidated marine deposits, composed of silt and clay, situated at the side of the dam. This erosion of the banks had for result that, after some time, the whole river was passing through this new channel, making the dam non-functional (Fig. 1).

We will suppose in this work that one already knows the state of the precipitation and we only look at the hydrological short term forecast. It is a difficult problem because one does not know exactly how to model the physical phenomena and one is unaware of the exact initial conditions of the system [5, 6]. The four-dimensional variational data assimilation (4D-VAR) consists in finding more relevant initial conditions by minimizing the error between the observations and the results of the simulation [7, 8, 9].

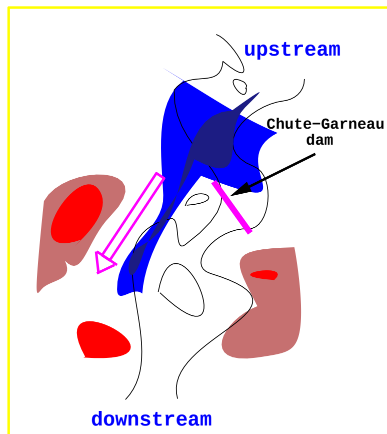

Figure 1: View of the Chute-Garneau dam after the flood (INRS-Eau, 1997).

We will first explain the 4D-VAR method in section 2. We then move on to introduce the problem cost function (section 3) and the minimization algorithm used to find its optimum (section 4). Then, sections 5 and 6 will present the 1D shallow-water equations with sediments and its corresponding adjoint equations, respectively. The same procedure is applied to the 2D shallow-water equations in section 7. The results and discussion are shown in section 8.

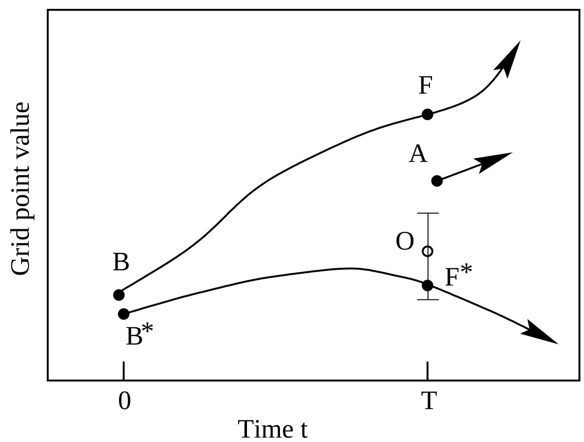

Figure 2: The 4D-VAR and how it works from Errico (1997).

2 THE 4D-VAR TECHNIQUE

An overview of the 4D-VAR technique is given by Fig. 2 where the point B is an estimate of the initial state of the system at the time 0. When we use the point B as being the initial state for the simulation, we obtain the point F at time T. This last point is located beyond the error of the observation O. We use the difference $F - O$ to produce a new initial state B^* at time 0. Moreover, B^* gives us a forecast F^* at the time T which is closer to the observations. Lastly, it was shown in the literature that for a time $t > T$, B^* will give us better results than B or another point A located between F and F^* [10].

We solve the direct problem by simulating the shallow-water equations with sediments [11]. Moreover, we design a cost function which represents the error between the results of the simulation and the observations. Then we determine, by a variational procedure, the set of adjoint equations which will be used to evaluate the gradient of this cost function. The cost function along with its gradient is passed to an minimization algorithm, such as the steepest descent, to find the optimal initial conditions.

3 THE COST FUNCTION

The 4D-VAR method consists in minimizing a cost function:

$$J = \int_{\Omega} \int_{0}^{T} f(\Psi, \vec{x}, t) \; d\vec{x} \; dt \qquad (1)$$

where $f(\Psi, \vec{x}, t)$ is a scalar function, defined over the time interval $[0, T]$ and a domain Ω. $f(\Psi, \vec{x}, t)$ is a model of the problem to solve [12].

The cost function can have different shapes. In data assimilation, the cost function measures the error between the simulated results and the observations [8] :

$$J = \frac{1}{2} \int_{\Omega} \int_{0}^{T} W(M(\Psi_0) - A_t)^2 \; d\vec{x} \; dt \qquad (2)$$

where W is a weight matrix containing the errors in the observations, i.e. $W = \frac{\text{signal}}{\text{noise}}$. $M(\Psi_0)$ is an operator modeling the evolution of an initial system state Ψ_0 toward a final state Ψ_t and A_t is the analysis (observations) taken at time t. On the other hand, in optimal control of airfoil design, one wants to minimize the drag coefficient, the lift-drag ratio and/or the targeted pressure distribution [13].

4 THE MINIMIZATION

To minimize the cost function, we have tested two optimization algorithms: steepest descent and quasi-Newton. Although the quasi-Newton converges quadratically, in our experiment we used the steepest descent method which converge linearly. This choice was made on the basis that the steepest descent will converge even if it is given a poor initial condition. The algorithm for the steepest descent is as follows. First, we evaluate the function (J) at the initial condition Ψ_0. Then we find the direction where the value of J will decreased ($-\nabla J$). We move in that direction by a reasonable distance and the new position becomes Ψ_1. Finally, we iterate until the gradient reaches the desired value [14].

5 THE SHALLOW-WATER EQUATIONS WITH SEDIMENTS IN 1D

The shallow-water equations are based on the mass conservation:

$$\frac{\partial h}{\partial t} + \frac{\partial hv}{\partial x} = 0, \qquad (3)$$

the momentum conservation:

$$\frac{\partial v}{\partial t} + v\frac{\partial v}{\partial x} + g\frac{\partial Z}{\partial x} + \frac{gv^2 n^2}{h^{\frac{4}{3}}} = 0, \qquad (4)$$

and a mass conservation for the sediments:

$$\frac{\partial}{\partial t}\left[(1-p)(Z_b - Z_s) + \frac{q_s}{v}\right] + \frac{\partial q_s}{\partial x} = 0. \qquad (5)$$

where $q_s = av^b$ is the sediment discharge (a and b are empirical constants), p is the sediment porosity, g is the gravitational acceleration and n is the Manning coefficient [15]. Figure 3 shows the reference used for the bathymetry where h is the water height, Z

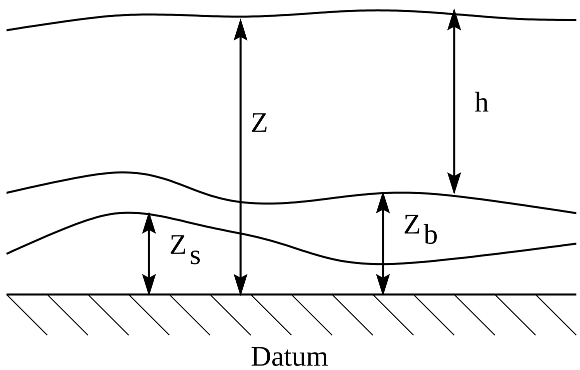

Figure 3: Reference used in the shallow-water equations.

is the total height, Z_s is the solid bed height (rock). The sediment layer thickness is given by $Z_b - Zs$. The datum is the reference level. To help with the linearization in the next section, we will rewrite Eq. 4 as:

$$\frac{\partial v}{\partial t} + \frac{1}{2}\frac{\partial v^2}{\partial x} + g\frac{\partial h}{\partial x} + g\frac{\partial z}{\partial x} + \frac{gv^2n^2}{h^{\frac{4}{3}}} = 0. \qquad (6)$$

Note that we have replaced the sediments height by z to simplify the notation. Moreover, in Eq. 5, we will substitute q_s for its value of av^b:

$$\frac{\partial}{\partial t}\left[(1-p)z + av^{b-1}\right] + a\frac{\partial v^b}{\partial x} = 0. \qquad (7)$$

6 THE ADJOINT EQUATIONS

6.1 Why do we need adjoint equations?

Since the equations are deterministic, the system state at some later time depends on its initial conditions $\Psi_t = M(\Psi_0)$ where Ψ is the state variables. We can therefore consider the cost function as a function of the initial conditions Ψ_0. In optimal theory, Ψ_0 is called the control variables as it is these variables which will be varied during the minimization process. We can also include the boundary conditions in the control variables [9]. Generally, the minimization algorithms need the gradient of the function to be minimized. Because the cost function is explicitly a function of the system state at the final time t and not of the initial conditions, the most efficient way to find the gradient ($\nabla_{\Psi_0} J$) of the cost function is to use the adjoint equations [7]. There are two main methods to find the adjoint equations: the lagrangian formulation, which we will use, and an inner product formulation [6, 16, 17].

6.2 The Lagrange formulation

The Lagrange undetermined multiplier formulation requires the construction of the Lagrangian:

$$\mathcal{L} = \int_\Omega \int_0^T J + \sum_{i=1}^{n} \lambda_i(\vec{x},t) g_i(\Psi,\vec{x},t)\ dt\ d\vec{x} \qquad (8)$$

where J is the cost function, $\lambda_i(\vec{x},t)$ is the undetermined multiplier and $g_i(\Psi,\vec{x},t)$ are the physical equations. Because $g_i(\Psi,\vec{x},t) = 0$, a minimization of $\mathcal{L}$ is equivalent to a minimization of J [12].

The Lagrangian for the one-dimensional shallow-water equations is:

$$\begin{aligned}
\mathcal{L} &= \int_0^T \int_0^L J + h^*[h_t + (hv)_x] \\
&+ v^*[v_t + (1/2)v_x^2 + gh_x + gz_x + gv^2n^2/h^{\frac{4}{3}}] \\
&+ z^*[(1-p)z_t + a(v^{b-1})_t + av_x^b]\ dx\ dt \qquad (9)
\end{aligned}$$

where h^*, v^* and z^* are the Lagrange multipliers or adjoint variables.

If we use integration by parts to pass the derivative operator from the real variables to the adjoint variables, we get:

$$\begin{aligned}
\mathcal{L} &= \int_0^T \int_0^L J - hh_t^* - hvh_x^* - vv_t^* \\
&- (1/2)v^2v_x^* - ghv_x^* - gzv_x^* + gv^2n^2v^*/h^{\frac{4}{3}} \\
&- (1-p)zz_t^* - av^{b-1}z_t^* - av^bz_x^*\ dx\ dt \\
&+ \int_0^L [h^*h + v^*v + z^*((1-p)z + av^{b-1})]|_0^T\ dx \\
&+ \int_0^T [h^*hv + v^*((1/2)v^2 + gh + gz) \\
&+ z^*av^b]|_0^L\ dt \qquad (10)
\end{aligned}$$

To find the stationary points (minima, maxima, saddle points), we apply to the Lagrangian the variational operator δ which explores the neighborhood of a state $\Psi = h, v, z$:

$$\begin{aligned}
\delta\mathcal{L} &= \int_0^T \int_0^L \delta h[J_h - h_t^* - vh_x^* - gv_x^* \\
&- (4/3)gv^2n^2v^*/h^{\frac{7}{3}}] + \delta v[J_v - hh_x^* - v_t^* - vv_x^* \\
&+ 2vgn^2v^*/h^{\frac{4}{3}} - a(b-1)v^{b-2}z_t^* - abv^{b-1}z_x^*] \\
&+ \delta z[J_z - gv_x^* - (1-p)z_t^*]\ dx\ dt \\
&+ \int_0^L [h^*\delta h + v^*\delta v + z^*((1-p)\delta z \\
&+ a(b-1)v^{b-2}\delta v)]|_0^T\ dx + \int_0^T [h^*(v\delta h + h\delta v) \\
&+ v^*(v\delta v + g\delta h + g\delta z) + abv^{b-1}z^*\delta v]|_0^L\ dt \qquad (11)
\end{aligned}$$

For an arbitrary non-zero displacement $(\delta h, \delta v, \delta z)$, we are at a minimum only if $\delta\mathcal{L} = 0$. This implies that we need to solve the adjoint equations:

$$h^*_\tau - vh^*_x - gv^*_x - (4/3)gv^2n^2v^*/h^{\frac{7}{3}} + J_h = 0 \quad (12)$$

$$\begin{aligned} v^*_\tau &- hh^*_x - vv^*_x + 2vgn^2v^*/h^{\frac{4}{3}} \\ &+ a(b-1)v^{b-2}z^*_\tau - abv^{b-1}z^*_x + J_v = 0 \end{aligned} \quad (13)$$

$$(1-p)z^*_\tau - gv^*_x + J_z = 0 \quad (14)$$

where the new variable $\tau = T - t$ is the inverse time. We select initial conditions and boundary conditions so that the two last integrals vanish. By using imposed boundary conditions [5], we get $h^*(\tau = T) = v^*(\tau = T) = z^*(\tau = T) = 0$ and $h^*(\tau = 0) = v^*(\tau = 0) = z^*(\tau = 0) = 0$ and $h^*(x = L) = v^*(x = L) = z^*(x = L) = 0$. We also obtain $\delta h(t = 0) = \delta v(t = 0) = \delta z(t = 0) = 0$, implying that the initial perturbation is null.

The adjoint equations are solved by iterating from $\tau = 0$ to $\tau = T$ in one time step: $d\tau = Nt \times dt$. In a general case, the cost function (Eq. 2) is:

$$\begin{aligned} J &= \frac{1}{2}\sum_{i=1}^{N_x}[W_h(h(T)_i - h_i^{obs})^2 + W_v(v(T)_i - v_i^{obs})^2 \\ &+ W_z(z(T)_i - z_i^{obs})^2]. \end{aligned} \quad (15)$$

We replaced the integrals by a sum over all the grid points because we discretized our problem. The difference between the final value of a quantity at each grid point (e.g. $h(T)$) and the observed quantity at each grid point (e.g. h^{obs}) is simply the error between the simulated quantity and the observed quantity. In our case, we chose to use $W_h = 0$, $W_v = 0$ and $W_z = 1$ because we decided to do data assimilation on the bathymetry only. This decision is due mainly because we do not have observations of the water height and speed. The gradient of the cost function is written in term of the adjoint variables at the time $\tau = T$. For example, ∇J with respect to h, evaluated at grid point i, is $h^*(\tau = T)_i$.

7 THE SHALLOW-WATER EQUATIONS AND ITS ADJOINT IN 2D

We may write the shallow-water equations as:

$$\frac{\partial P}{\partial t} + \vec{\nabla}\cdot(P\vec{V}) = 0 \quad (16)$$

$$\frac{\partial \vec{V}}{\partial t} + \eta\vec{N} \times (P\vec{V}) + \vec{\nabla}\left(P + \frac{\vec{V}\cdot\vec{V}}{2}\right) = 0 \quad (17)$$

where P is the hydrostatic pressure and the potential vorticity is written $\eta = \frac{\vec{\nabla}\times\vec{V}}{P}$ [18]. In order to include the sediments, we change in Eq. 17 the pressure P by $(H + Z_b)g$ where H is the water height and Z_b is the bathymetry. We obtain:

$$\begin{aligned} \frac{\partial \vec{V}}{\partial t} &+ \eta\vec{N} \times ((H + Z_b)g\vec{V}) \\ &+ \vec{\nabla}\left((H + Z_b)g + \frac{\vec{V}\cdot\vec{V}}{2}\right) \\ &+ \frac{gn^2 \parallel \vec{V} \parallel \vec{V}}{h^{\frac{4}{3}}} = 0 \end{aligned} \quad (18)$$

with $\eta = \frac{\vec{\nabla}\times\vec{V}}{(H+Z_b)g}$. We also added a Manning friction term. The equation for the mobile bathymetry is:

$$\frac{\partial}{\partial t}\left[(1-p)Z_b + \frac{\parallel \vec{q}_s \parallel}{\parallel \vec{V} \parallel}\right] + \vec{\nabla}\cdot\vec{q}_s = 0. \quad (19)$$

The sediment discharge was modeled by $\vec{q}_s = \frac{a\|\vec{V}\|^2}{H^b}$. By following the method presented in section 6, we find that the adjoint equations are:

$$\begin{aligned} h^*_\tau &- uh^*_x - vh^*_y - g(u^*_x + v^*_y) - \frac{ab}{h^{b+1}}\sqrt{\frac{u^4+v^4}{u^2+v^2}}z^*_\tau \\ &- \frac{4}{3}\frac{gn^2}{h^{\frac{7}{3}}}\sqrt{u^2+v^2}(uu^* + vv^*) \\ &+ \frac{ab}{h^{b+1}}(u^2z^*_x + v^2z^*_y) + J_h = 0 \end{aligned} \quad (20)$$

$$\begin{aligned} u^*_\tau &- hh^*_x - uu^*_x + wv^* - uv^*_y + \frac{au}{h^b}Cz^*_\tau - \frac{2au}{h^b}z^*_x \\ &+ u^*\frac{gn^2}{h^{\frac{4}{3}}}\frac{2u^2+v^2}{\sqrt{u^2+v^2}} + v^*\frac{gn^2vu}{h^{\frac{4}{3}}}\sqrt{u^2+v^2} \\ &+ J_u = 0 \end{aligned} \quad (21)$$

$$\begin{aligned} v^*_\tau &- hh^*_y - vu^*_x - wu^* - vv^*_y + \frac{av}{h^b}Cz^*_\tau - \frac{2av}{h^b}z^*_y \\ &+ u^*\frac{gn^2vu}{h^{\frac{4}{3}}}\sqrt{u^2+v^2} + v^*\frac{gn^2}{h^{\frac{4}{3}}}\frac{u^2+2v^2}{\sqrt{u^2+v^2}} \\ &+ J_v = 0 \end{aligned} \quad (22)$$

$$(1-p)z^*_\tau - g(u^*_x + v^*_y) + J_z = 0 \quad (23)$$

with $w = \frac{\partial v}{\partial x} - \frac{\partial u}{\partial y}$, $C = \frac{u^4+2u^2v^2-v^4}{(u^2+v^2)^2}\sqrt{\frac{u^2+v^2}{u^4+v^4}}$ and $\tau = T - t$. The initial conditions and boundary conditions are found the same way as the 1D case.

8 THE DEGRADATION EXPERIMENT

We tested the 4D-VAR on a degradation (erosion) experiment carried in a flume by Bhallamudi and

Chaudhry in 1991 [15]. A small stream of water ($q_0 = 0.0028\ m^2/s$, $h_0 = 0.0305\ m$), flows on a bed of sand. After some time (2 hours 40 min.), the sediments in the bed will be displaced and we want to recreate the measured observations with our shallow-water model. As shown in Fig. 4, the water

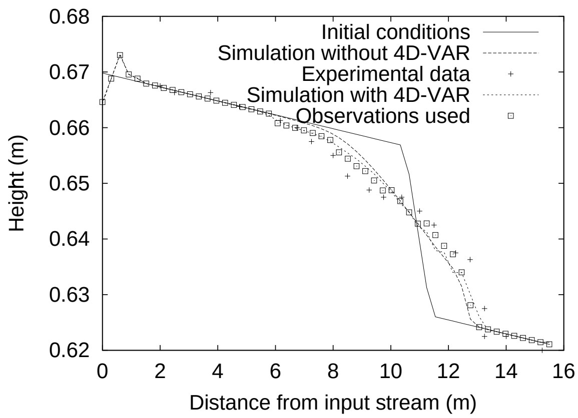

Figure 4: Alluvial degradation. Experimental data are from Bhallamudi and Chaudhry (1991). [15]

smoothened the sharp edge of the bed. We can see from the experimental data that the shallow-water model did not eroded enough sand at 7 to 10 m from the stream. This causes a smaller accumulation of sand at the bottom of the step. If we use the 4D-VAR method with the experimental data, the steep slope develops discontinuities. We used instead a set of observations with similar characteristics as the lab data. With these observations, we see that the 4D-VAR algorithm has a tendency to amplify the observations by digging deeper uphill and moving more sand downhill.

We plotted on Fig. 5 the original initial conditions with the 4D-VAR modified initial conditions. This is the *initial conditions* we need to use to obtain the smallest error between the results of the simulation and the observations. We notice that it behaves like the observations. The 4D-VAR helps the shallow-water code by hinting it what to do.

Figure 6 shows the error for the case when 4D-VAR is used and when it is not used. With 4D-VAR, the error in the 6 to 10 m interval is greatly reduced. The smallest reduction in this interval is about half the error, which is acceptable. In the interval 11 to 13 m, the results are less notable as for some points the error is reduced while for the other ones it has slightly increased.

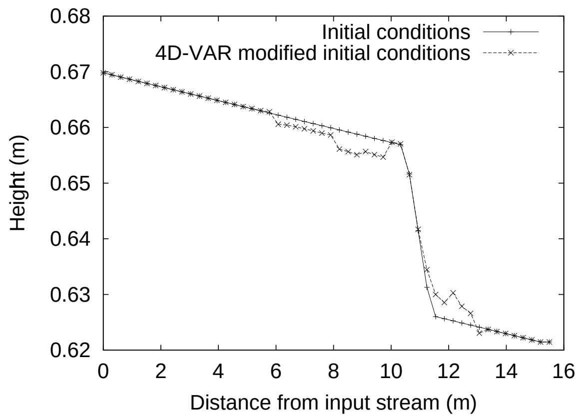

Figure 5: Comparison of the initial conditions with the 4D-VAR modified initial conditions. It is seen that, to get the minimal error between the results of the simulation and the observations, the 4D-VAR insists that the initial conditions must have common feature with the observations (Figure 4).

9 CONCLUSION

In this work, we have given a detailed explanation of the 4D-VAR data assimilation method in the case of shallow-water. In particular, we showed how to derive the adjoint equations of the model. A degradation example was used to get insight about the method's efficiency. This example was chosen because the phenomenon of degradation is very important in the investigation of a two-dimensional river bed. From this example, we have learned that the optimal initial conditions has some resemblance with the observations. Moreover, the 4D-VAR method is successful in reducing the error between the results and the observations.

More advanced 2D data assimilation results are on the way and will be presented at the conference. We are currently studying the case of the Chicoutimi River [4].

10 ACKNOWLEDGMENTS

This work has been done as a part of the RCM2 project: *Nowcasting And Decision Making For Environmental Problems.* The computations have been made at CERCA on a SGI R10000 workstation. We would like to thanks Marilène Gagnon from CERCA and Gilbert Brunet from RPN, Dorval for their useful discussions. Special thanks goes to Pr. H. Chaudhry for kindly giving us the permission to use his experimental data.

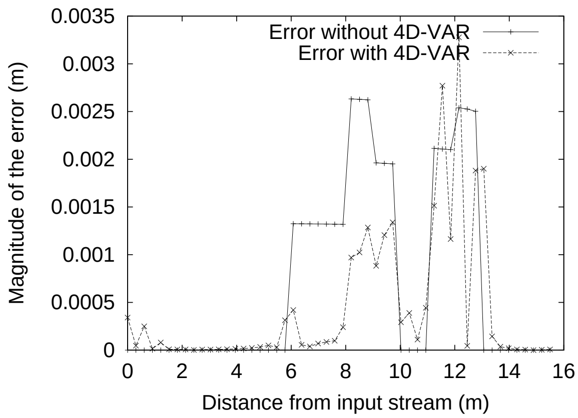

Figure 6: Magnitude of the error between the results of the simulation and the observations. We compare the error when we do not use 4D-VAR against the case where 4D-VAR is used. For the bed situated at 6 to 10 m from the stream, 4D-VAR reduces the error. Further downstream, the 4D-VAR method is less effective.

11 REFERENCES

[1] Chaudhry, M. H. *Open-Channel Flow.* Englewood Cliffs, New Jersey: Prentice-Hall, 1993.

[2] Brooks, G. R. and D. E. Lawrence, "Geomorphic effects of flooding along reaches of selected rivers in the Saguenay region, Québec, July 1996," *Géographie physique et Quaternaire*, vol. 54, no. 3, pp. 281–299, 2000.

[3] Nicolet, R., L. Roy, R. Arès, J. Dufour, G. Marinier, and G. Morin, "Rapport : Commission scientifique et technique sur la gestion de barrages," tech. rep., Québec, 1997.

[4] INRS-Eau, "Simulation hydrodynamique et bilan sédimentaire des rivières chicoutimi et des Ha! Ha! suite aux crues exceptionnelles de juillet 1996," Jan. 1997. Rapport INRS-Eau No. R487, http://www.inrs-eau.uquebec.ca/saguenay/.

[5] Daley, R. *Atmospheric Data Analysis.* Cambridge atmospheric and space science series, Cambridge: Cambridge University Press, 1991.

[6] Le Dimet, F.-X. and O. Talagrand, "Variational algorithms for analysis and assimilation of meteorological observations: theoretical aspects," *Tellus*, vol. 38A, pp. 97–110, 1986.

[7] Courtier, P. and O. Talagrand, "Variational assimilation of meteorological observations with the direct and adjoint shallow-water equations," *Tellus*, vol. 42A, pp. 531–549, 1990.

[8] Talagrand, O. and P. Courtier, "Variational assimilation of meteorological observations with the adjoint vorticity equation. I: Theory," *Q. J. R. Meteorol. Soc.*, vol. 113, pp. 1311–1328, 1987.

[9] Wenzel, M. *Adjoint Method (4D-VAR).* The Alfred Wegener Institute Foundation for Polar and Marine Research, 2001. http://e-net.awi-bremerhaven.de/Modelling/INVERSE/adjoint.html.

[10] Errico, R. M., "What is an adjoint model?," *Bulletin of the American Meteorological Society*, vol. 78, pp. 2577–2591, Nov. 1997.

[11] Fortin, A. and A. Vincent, "Dam break with sediment transport," in *The Ninth Annual Conference of the CFD Society of Canada* (G. E. Schneider, ed.), pp. 237–241, 2001.

[12] Sanders, B. F. and N. D. Katopodes, "Adjoint sensitivity analysis for shallow-water wave control," *Journal of Engineering Mechanics*, vol. 126, pp. 909–919, September 2000.

[13] Nadarajah, S. K. and A. Jameson, "A comparison of the continuous and discrete adjoint approach to automatic aerodynamic optimization," in *AIAA-2000-0667*, AIAA 38th Aerospace Sciences Meeting and Exhibit,, (Reno, Nevada), Jan. 2000.

[14] Burden, R. L. and J. D. Faires. *Numerical Analysis.* Boston: PWS Publishing Company, 1993.

[15] Bhallamudi, S. M. and M. H. Chaudhry, "Numerical modeling of aggradation and degradation in alluvial channels," *Journal of Hydraulic Engineering*, vol. 117, no. 9, pp. 1145–1164, 1991.

[16] Bewley T. R., "Flow control: new challenges for a new Renaissance," *Progress in Aerospace Sciences*, vol. 37, no. 1, pp. 21–58, 2001.

[17] Bewley, T. R., P. Moin, and R. Temam, "DNS-based predictive control of turbulence: an optimal benchmark for feedback algorithms," *Journal of Fluid Mechanics*, vol. 447, pp. 179–225, 2001.

[18] Sadourny, R., "The dynamics of finite-difference models of the shallow-water equations," *Journal of the Atmospheric Sciences*, vol. 32, pp. 680–689, April 1975.